

Figure 3–Figure Supplement 1

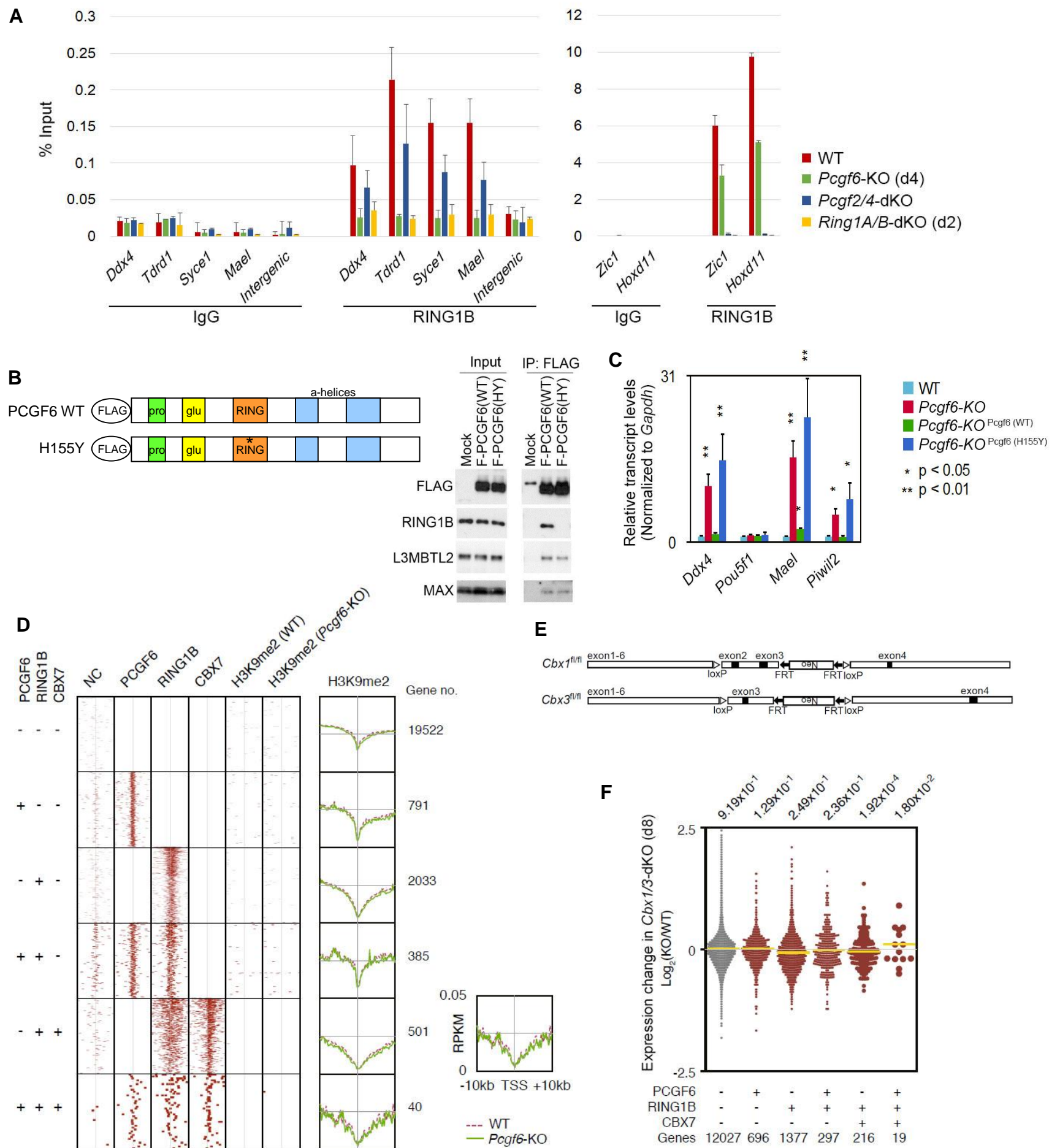


Figure 3–Figure Supplement 1. The role of PCGF6 in recruiting PCGF6-PRC1 to its target genes.

(A) Changes in local RING1B deposition at selected PCGF6-PRC1 target genes in WT, *Pcgf6*-KO, *Pcgf2/4*-dKO, and *Ring1A/B*-dKO ESCs are shown as described in Figure 2C. (B) The expression of a 3xFLAG -tagged wild type or mutant PCGF6 in *Pcgf6*-KO ESCs. Schematic representation for wild type (WT) and a H155Y mutant (HY) (top). The constructs were stably expressed in *Pcgf6*^{fl/fl}; *Rosa26*::*CreERT2*^{tg/+} ESCs. Immunoprecipitation-Immunoblotting (IP-IB) analysis revealed the association of exogenous PCGF6 WT and HY with endogenous L3MBTL2 and MAX while PCGF6 HY failed to associate with RING1B. Extracts of OHT-untreated *Pcgf6*^{fl/fl}; *Rosa26*::*CreERT2*^{tg/+} ESC lines expressing either construct were IPed with anti-FLAG antibody. IP (IP) and lysates (Input) were immunoblotted with antibodies against FLAG, RING1B, L3MBTL2 or MAX. (C) Expression levels of the indicated genes in wild type (WT) or *Pcgf6*-KO ESCs stably expressing wild type [*Pcgf6* (WT)] or H155Y mutant [*Pcgf6* (H155Y)]. Expression levels were normalized to a *Gapdh* control and are depicted as fold change relative to wild type ESCs. Error bars represent standard deviation determined from at least three independent experiments. The *p*-values for the expression changes induced by *Pcgf6* deletion were calculated by the Student's *t*-test. (D) A heat map view for distribution of H3K9me2 in ± 10 kb genomic regions around transcription start sites (TSS) in wild type (WT) and *Pcgf6*-KO ESCs is shown as described in Figure 1G. The distribution of PCGF6, RING1B, CBX7 is also shown. (E) Schematic representation of the construct for conditional targeting of *Cbx1* and *Cbx3* loci is shown as described in Figure 1–Figure Supplement 1A. (F) Gene expression changes in *Cbx1/3*-dKO ESCs are shown as described in Figure 1–Figure Supplement 1G.